Controllable Synthesis of Uniform Mesoporous H-Nb_2O_5/rGO Nanocomposites for Advanced Lithium Ion Hybrid Supercapacitor

Electronic Supplementary Information

Shengyuan Li, ‡[a] Ting Wang, ‡[cd] Wangqin Zhu,[a] Jiabiao Lian,*[a] Yunpeng Huang,[a] Yangyang Yu,[b] Jingxia Qiu, [a] Yan Zhao, [a] Yang-Chun Yong *[b] and Huaming Li [a]

[a] Key Laboratory of Zhenjiang, Institute for Energy Research, Jiangsu University, Zhenjiang 212013, P. R. China

[b] Biofuels Institute, Jiangsu University, Zhenjiang 212013, P. R. China

[c] Nanyang Environment and Water Research Institute (NEWRI), Interdisciplinary Graduate School (IGS), Nanyang Technological University, Cleantech One, 637141 Singapore

[d] School of Materials Science and Engineering, Nanyang Technological University, 50 Nanyang Avenue, 639798, Singapore

‡ S. Y. Li and T. Wang contributed equally to this work.

* Corresponding authors: Tel/Fax: 0086-511-88799500. *E-mail address*: jblian@ujs.edu.cn (J. B. Lian); ycyong@ujs.edu.cn (Y. C. Yong).

Fig. S1 FTIR spectra of the as-prepared GO nanosheets (a), H-Nb_2O_5/GO nanocomposites (b), and H-Nb_2O_5/rGO nanocomposites (c).

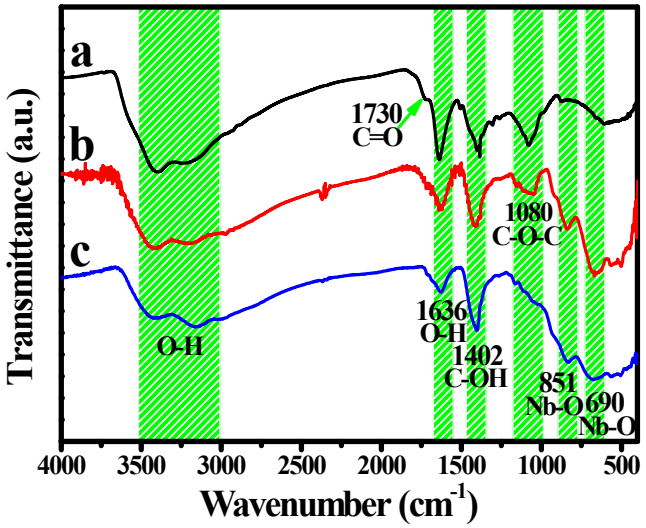

The FT-IR spectrum of GO (Figure S1a) indicates the presence of C−O−C (ν_{C-O-C} at 1080 cm^{-1}), C−OH (ν_{C-OH} at 1402 cm^{-1}), C=O in carboxylic acid and carbonyl moieties ($\nu_{C=O}$ at 1730 cm^{-1}). The broad absorption peak between 3000 and 3500 cm^{-1} is due to the presence of surface hydroxyl groups, and a peak at 1636 cm^{-1} is attributed assigned to the bending vibration of water molecules. As shown in the FT-IR spectra of nanocomposites (Figure S1b and S1c), there are two new peaks at 690 and 851 cm^{-1}, which are the Nb–O characteristic vibrations, demonstrating well complexation of Nb_2O_5 and GO or rGO in the nanocomposites. Moreover, compared with the curve b, the peaks of C−O−C and C=O are absent in curve c, indicating the successful deoxygenation of GO during the annealing process.

As mentioned above, the FT-IR results are in good accordance with the Raman and XPS analyses in the main text, which further demonstrate that: (i) the as-prepared GO nanosheets contain many functional groups, including C−O−C, −COOH, C=O, and −OH; (ii) the successful combination of Nb_2O_5 with GO; and (iii) the effective reduction of GO to rGO in the nanocomposites by annealing.

Fig. S2 C 1s (top) and O1s (bottom) core level XPS spectra of GO nanosheets.

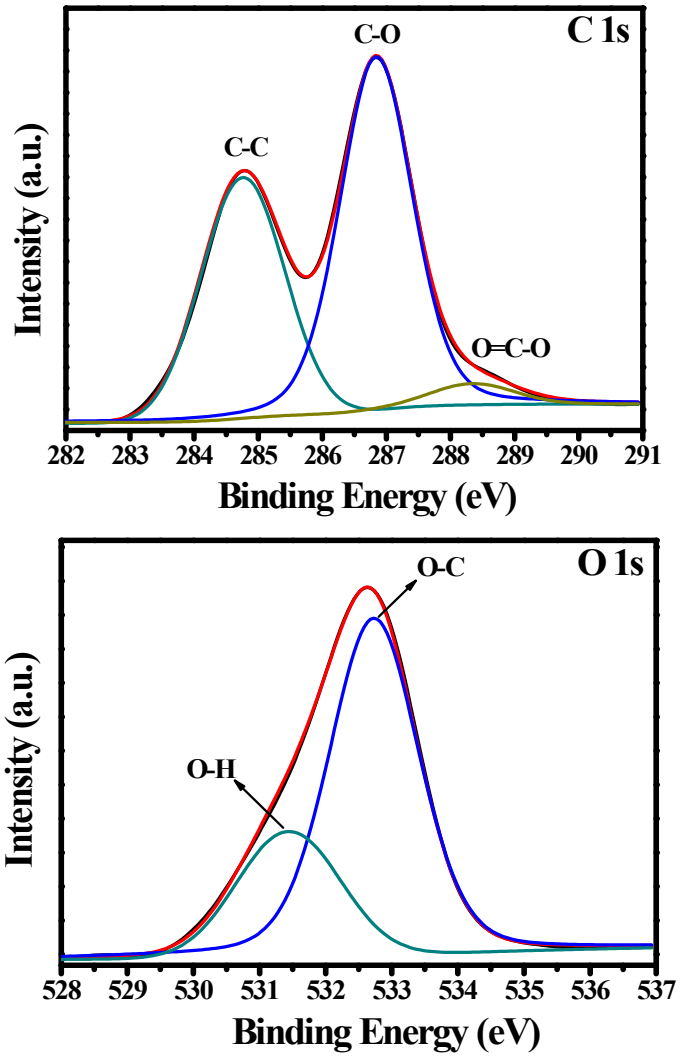

Fig. S3 STEM images and EDX elemental mapping images of the as-prepared H-Nb_2O_5 microflowers composed of nanoflakes (top), H-Nb_2O_5/GO nanocomposites (middle), and H-Nb_2O_5/rGO nanocomposites (bottom), respectively.

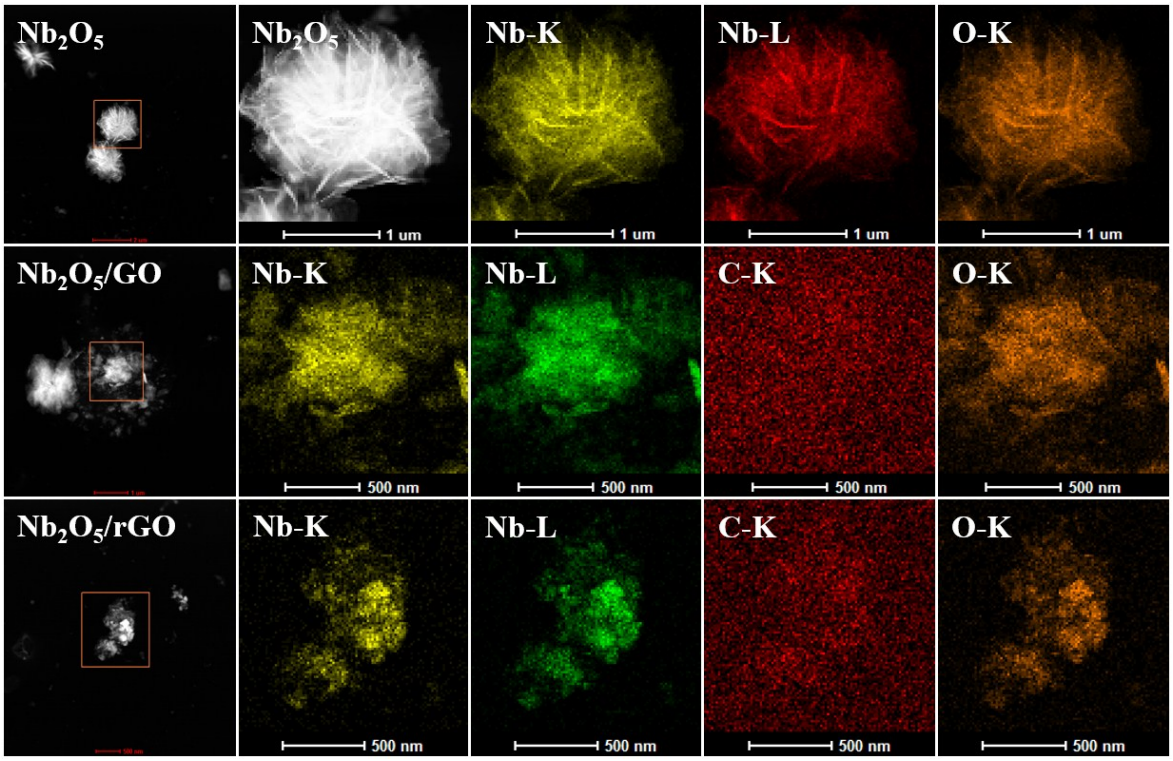

Fig. S4 FE-SEM images of the as-prepared $Zn_2Ti_3O_8$/rGO (a), Si/rGO (b), $NaNbO_3$/rGO (c), Nb_4N_5/rGO (d), and H-Nb_2O_5/2D g-C_3N_4 nanocomposites (e and f), respectively.

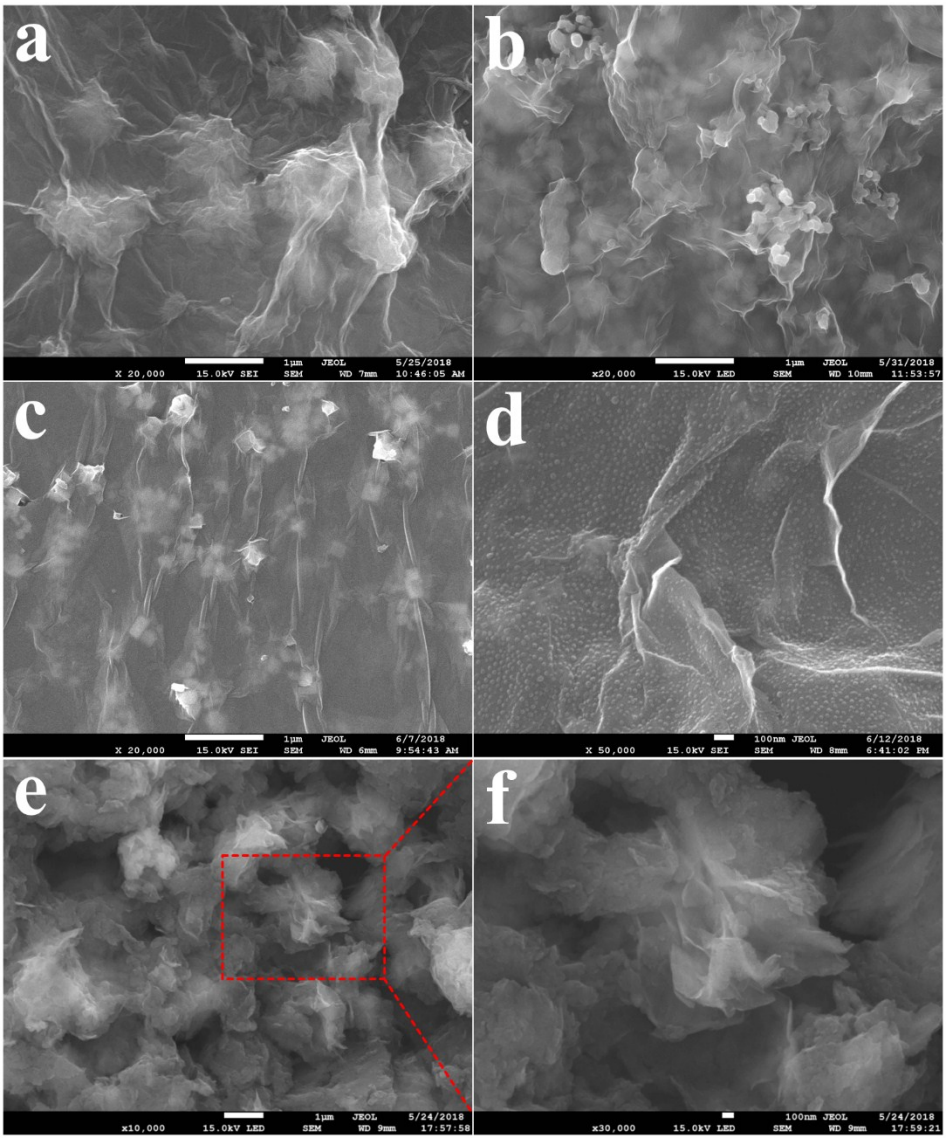

Fig. S5 Low- and high-magnification FE-SEM images of the pristine H-Nb_2O_5 electrode (a and b) and H-Nb_2O_5/rGO nanocomposite electrode (c and d) after cycling for 500 times.

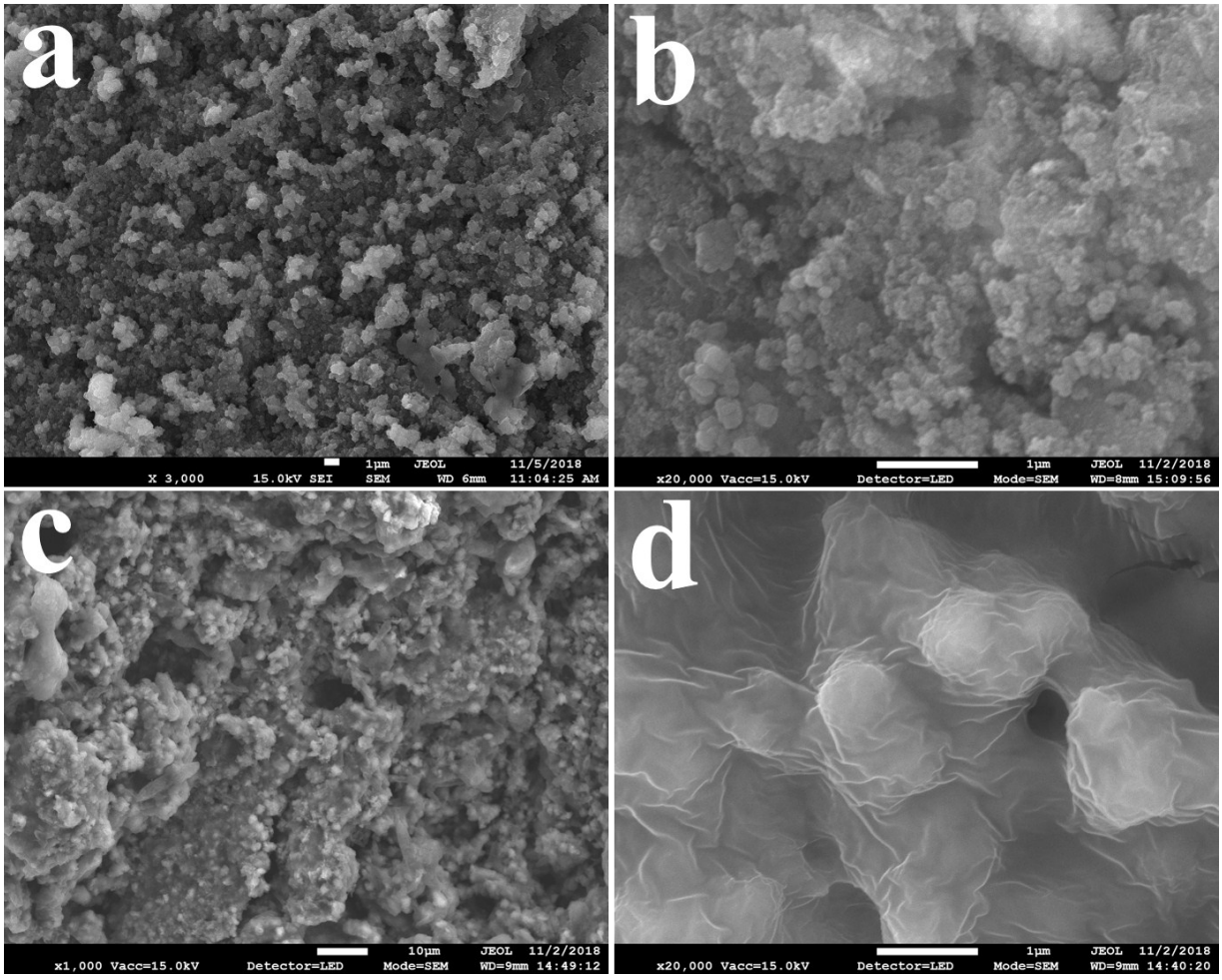

Fig. S6 (a) Nitrogen adsorption–desorption isothermal and the BJH pore size distribution curves (inset) of the SCCB nanopowders. Electrochemical performance of the SCCB nanopowder electrode in a half cell between 3.0 and 4.5 V vs. Li/Li^+ in the 1 M $LiPF_6$ electrolyte: (b) CV curves at different sweep rates ranging from 1.0 mV s^{-1} to 50 mV s^{-1}; (c) Galvanostatic charge-discharge curves at different current densities of 0.1−5.0 A g^{-1}; (d) Gravimetric capacitance as a function of current density; (e) Cycling performance at the current density of 1.0 A g^{-1}.

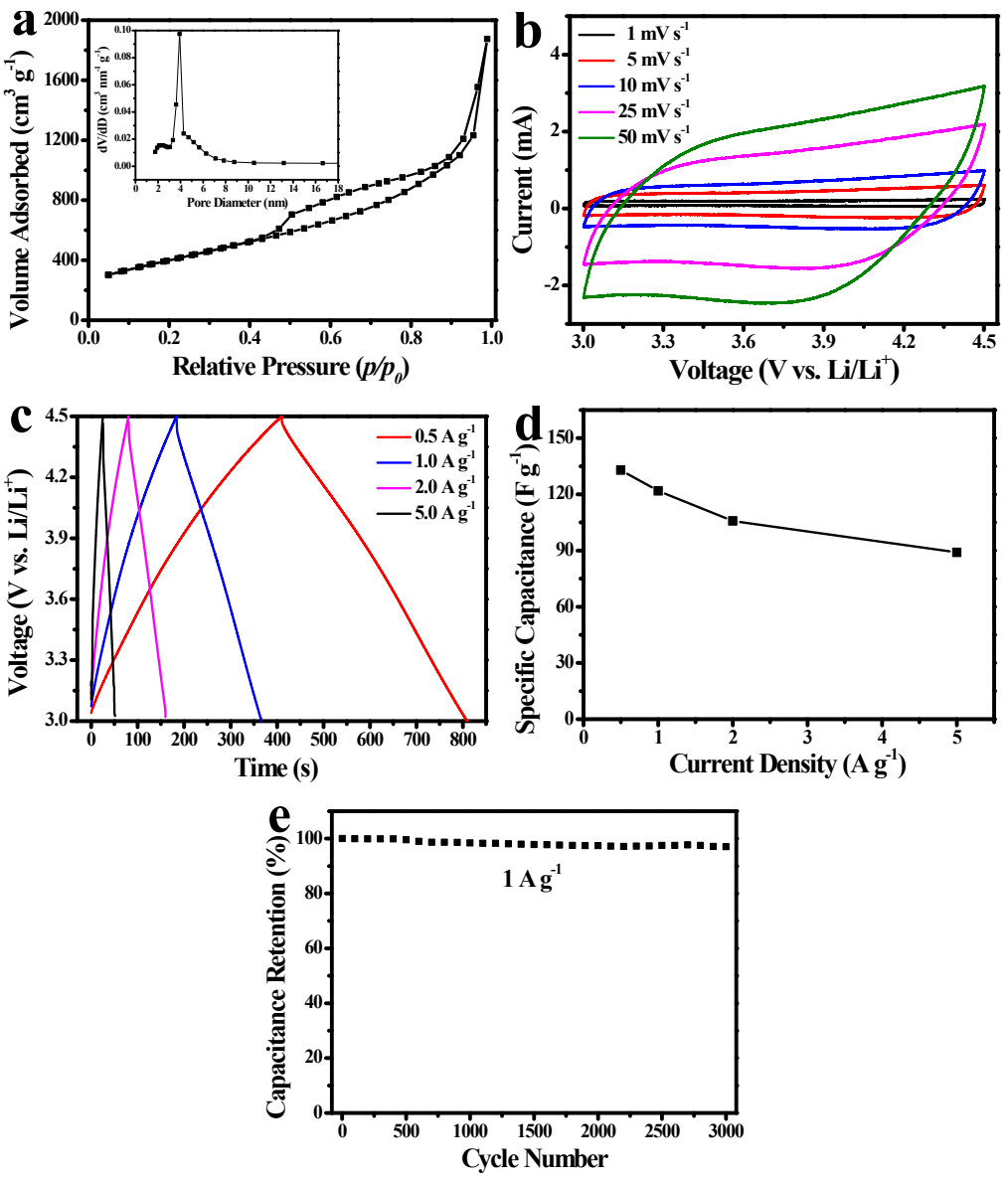

To design and assemble a high performance LIHS, the commercial super conductive carbon black (SCCB) nanopowder was chosen as cathode to couple with the pre-lithiated H-Nb_2O_5/rGO anode. Fig. S6a shows the nitrogen adsorption–desorption isothermal and its corresponding BJH pore size distribution curves (inset) of the SCCB nanopowders, indicating large specific surface area (S_{BET}) of 1439 m^2 g^{-1} and mesoporous structure with the main pore size distribution of 4 nm. Fig. S6b shows the CV curves of SCCB nanopowder in the potential range of 3.0−4.5 V (vs. Li/Li^+) at different scanning rates from 1.0 to 50 mV s^{-1}, which exhibit typical rectangular shape, indicating its superior electrical double-layer characteristic. The galvanostatic charge-discharge (GCD) curves at various current densities (Fig. S6c) exhibit excellent symmetry, revealing its good reversibility. Its specific capacitance is calculated to be 132 F g^{-1} (corresponding to 55 mAh g^{-1}) at a current density of 0.5 A g^{-1}, and still remains 89 F g^{-1} at a high current density of 5.0 A g^{-1}, as shown in Fig. S6d. More importantly, the SCCB electrode exhibits outstanding cycling stability with 97% capacitance retention after 3000 cycles at 1.0 A g^{-1}, as shown in Fig. S6e. These results reveal that the SCCB nanopowder has high specific capacitance, remarkable rate capability, and long cycle life, which is very suitable for high-performance hybrid capacitors.

Fig. S7 Nyquist plot with the fitted impedance data plotted by solid line and the equivalent electrical circuit model of the H-Nb_2O_5/rGO//SCCB LIHS.

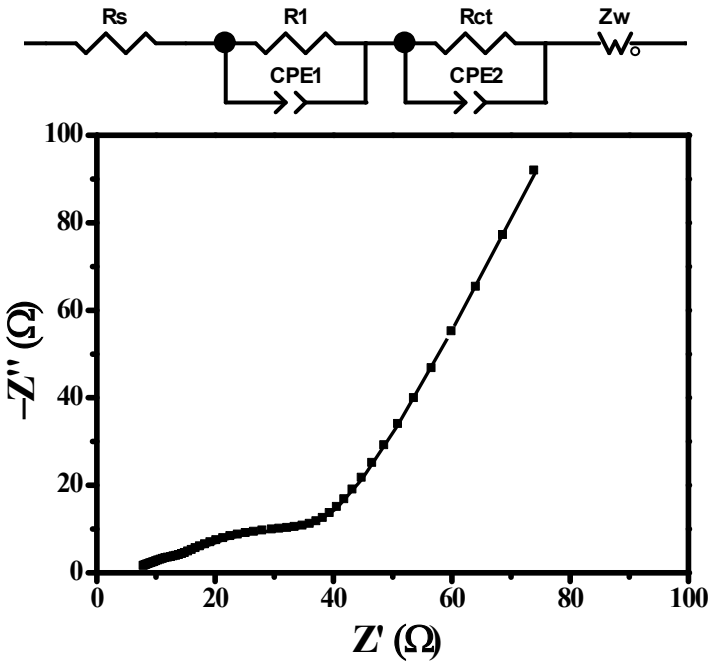

Table S1 The parameters derived from the fitted data of Nyquist plots using ZView software.

Sample	H-Nb_2O_5 electrode	H-Nb_2O_5/rGO electrode	H-Nb_2O_5/rGO//SCCB LIHS
R_s (Ω)	11.6	2.8	6.3
R_1 (Ω)	44.2	6.9	8.1
R_{ct} (Ω)	86.4	11.7	31.5

Table S2 Electrochemical performance of our H-Nb_2O_5/rGO//SCCB LIHS in comparison with other previously reported hybrid supercapacitors.

Anode//Cathode [Reference]	Energy Density (W h kg^{-1})	Power Density (W kg^{-1})	Cycling Life
H-Nb_2O_5/rGO//SCCB Present work	**100.2**	**20000**	**82%@3000 cycles**
T-Nb_2O_5@C//MSP-20 [1]	63	16528	~90%@1000 cycles
M-Nb_2O_5-C//AC [2]	74	18510	90%@1000 cycles
T-Nb_2O_5/graphene//AC [3]	47	18000	93%@2000 cycles
CNTs/Nb_2O_5//AC [4]	33.5	4000	Nil
Nb_2O_5//AC [5]	95.55	5350.9	81%@1000 cycles
Nb_2O_5@C/rGO//AC [6]	76	20800	~100%@3000 cycles
T-Nb_2O_5/rGO//AC [7]	45.1	9100	82%@5000 cycles
TNO@C//CFs [8]	110.4	5464	77%@1500 cycles
$TiNb_2O_7$//graphene [9]	74	7500	81.25%@3000 cycles
TiO_2/CNT//AC/CNT[10]	104	5000	71%@2000 cycles
TiO_2@EEG//EEG [11]	72	2000	68%@500 cycles
TiC//PHPNC [12]	101.5	67500	82%@5000 cycles

References:

1. E. Lim, C. Jo, H. Kim, H. Kim, Y. Mun, J. Chun, Y. Ye, K. Ha, K. C. Roh, K. Kang, S. Yoon and J. Lee, *ACS Nano*, 2015, **9**, 7497–7505.
2. E. Lim, H. Kim, C. Jo, J. Chun, K. Ku, S. Kin, H. Lee, I. Nam, S. Yoon, K. Kang and J. Lee, *ACS Nano*, 2014, **8**, 8968–8978.
3. L. P. Kong, C. F. Zhang, J. T. Wang, W. M. Qiao, L. C. Ling and D. H. Long, *ACS Nano*, 2015, **9**, 11200–11208.
4. X. L. Wang, G. Li, Z. Chen, V. Augustyn, X. M. Ma, G. Wang, B. Dunn and Y. F. Lu, *Adv. Energy Mater.*, 2011, **1**, 1089–1093.
5. B. H. Deng, T. Y. Lei, W. H. Zhu, L. Xiao and J. P. Liu, *Adv. Funct. Mater.* 2018, **28**, 1704330.
6. E. Lim, C. Jo, M. S. Kim, M. H. Kim, J. Chun, H. Kim, J. Park, K. C. Roh, K. Kang and S. Yoon, *Adv. Funct. Mater.* 2016, **26**, 3711−3719.
7. Y. Z. Jiao, H. T. Zhang, H. L. Zhang, A. Liu, Y. X. Liu and S. J. Zhang, *Nano Res.*, 2018, **11**, 4673−4685.
8. X. F. Wang and G. Z. Shen, *Nano Energy* 2015, **15**, 104−115.

9. H. S. Li, L. F. Shen, J. Wang, S. Fang, Y. X. Zhang, H. Dou and X. G. Zhang, *J. Mater. Chem. A* 2015, **3**, 16785−16790.
10. L. F. Que, F. D. Yu, Z. B. Wang and D. M. Gu, *Small* 2018, **14**, 1704508.
11. F. X. Wang, C. Wang, Y. J. Zhao, Z. C. Liu, Z. Chang, L. J. Fu, Y. S. Zhu, Y. P. Wu and D. Y. Zhao, *Small* 2016, **12**, 6207−6213.
12. H. W. Wang, Y. Zhang, H. X. Ang, Y. Q. Zhang, H. T. Tan, Y. F. Zhang, Y. Y. Guo, J. B. Franklin, X. L. Wu, M. Srinivasan, H. J. Fan and Q. Y. Yan, *Adv. Funct. Mater.* 2016, **26**, 3082−3093.